

# $k$ -commutativity and measurement reduction for expectation values

Ben DalFavero,<sup>1</sup> Rahul Sarkar,<sup>2</sup> Daan Camps,<sup>3</sup> Nicolas Sawaya,<sup>4</sup> Ryan LaRose<sup>1,\*</sup>

<sup>1</sup>*Center for Quantum Computing, Science, and Engineering,  
Michigan State University, East Lansing, MI 48823, USA*

<sup>2</sup>*Institute for Computational & Mathematical Engineering, Stanford University, USA*

<sup>3</sup>*National Energy Research Scientific Computing Center,  
Lawrence Berkeley National Laboratory, Berkeley, California, USA*

<sup>4</sup>*HPI Biosciences, Oakland, CA 94608; and Azulene Labs Inc., San Francisco, CA 94115*

We introduce a notion of commutativity between operators on a tensor product space, nominally Pauli strings on qubits, that interpolates between qubit-wise commutativity and (full) commutativity. We apply this notion, which we call  $k$ -commutativity, to measuring expectation values of observables in quantum circuits and show a reduction in the number measurements at the cost of increased circuit depth. Last, we discuss the asymptotic measurement complexity of  $k$ -commutativity for several families of  $n$ -qubit Hamiltonians, showing examples with  $O(1)$ ,  $O(\sqrt{n})$ , and  $O(n)$  scaling.

## I. INTRODUCTION

A fundamental task in quantum information is measuring the expectation value of a Hermitian operator  $H$  in a state  $|\psi\rangle$ , i.e., evaluating or estimating

$$\langle\psi|H|\psi\rangle. \quad (1)$$

For simplicity we refer to this as “measuring  $H$ .” Without loss of generality we take  $H$  to be an  $n$ -qubit Hamiltonian written as a linear combination of Pauli strings

$$H = \sum_{\alpha} c^{[\alpha]} P^{[\alpha]} \quad (2)$$

where each  $c^{[\alpha]}$  is a real coefficient and each  $P^{[\alpha]}$  is a tensor product of  $n$  Paulis  $I$ ,  $X$ ,  $Y$ , or  $Z$ . We use superscripts (e.g.,  $P^{[\alpha]}$  and  $P^{[\beta]}$ ) or different symbols (e.g.,  $P$  and  $Q$ ) to indicate different Pauli strings, and we use subscripts to indicate the (qubit) support of Pauli strings (e.g., for  $P = XYZ$ ,  $P_0 = X$ ,  $P_1 = Y$ , and  $P_2 = Z$ ).

For any mutually commuting set of  $n$ -qubit Pauli strings  $\{P^{[\alpha]}\}_{\alpha}$ , there exists a Clifford unitary  $U$  such that  $UP^{[\alpha]}U^{\dagger}$  is diagonal for every  $\alpha$ . Measuring  $\{P^{[\alpha]}\}_{\alpha}$  can thus be accomplished in a single circuit by appending  $U$  to the circuit that prepares  $|\psi\rangle$  then measuring in the computational basis. Ref. [1] showed that  $U$  can be implemented in  $O(n^2/\log n)$  Clifford gates. For  $r \leq n$  independent Paulis, Ref. [2] showed that  $U$  can be implemented in  $O(rn/\log r)$  two-qubit Clifford gates. Several algorithms have been developed for efficiently compiling such Clifford circuits [3–5].

Motivated by the desire to have short-depth circuits due to hardware constraints, the notion of qubit-wise commutativity was developed [6] (and even prior to this reference under the name of “tensor product basis sets” [7], although the term qubit-wise commutativity is most commonly used). Two Pauli strings  $P$  and  $Q$

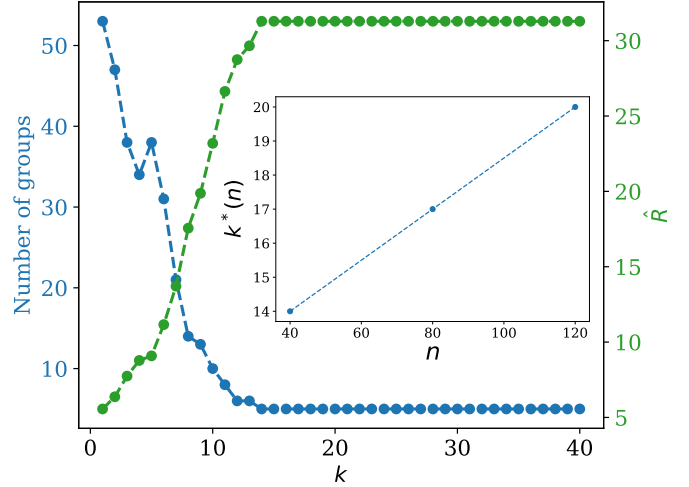


FIG. 1. Measuring an  $n = 40$  qubit spinless, two-dimensional Fermi-Hubbard Hamiltonian (5) by grouping terms into  $k$ -commuting sets for  $1 \leq k \leq n$ . The left axis (blue) shows the number of groups as a function of  $k$  and the right axis (green) shows  $\hat{R}$  defined in (6) as a function of  $k$ . As can be seen, the number of groups generally decreases as  $k$  increases, and  $\hat{R}$  increases as  $k$  increases. Additionally, the plot shows a value  $k^* < n$  at which  $\hat{R}$  saturates. The inset shows this value  $k^*(n)$  as a function of system size for  $n = 40, 80$ , and  $120$  qubit Fermi-Hubbard Hamiltonians for which we see linear scaling.

are said to qubit-wise commute if  $[P_i, Q_i] = 0$  for all  $i \in [n]$ . If  $P$  and  $Q$  qubit-wise commute, they can be measured together in a depth-one quantum circuit. The catch is that, given a generic Hamiltonian (2), not all Pauli strings will qubit-wise commute. Approximate optimization algorithms are employed to group Paulis into qubit-wise commuting sets such that each set can be measured with a single depth-one circuit. This provides a trade off, decreasing circuit depth at the cost of increasing the number of circuits needed to be run.

Thus there are two notions of commutativity used in measuring  $n$ -qubit Hamiltonians: qubit-wise commuting which results in  $N \geq 1$  circuits of additional depth  $d = 1$ , and fully commuting which results in  $N = 1$  circuit of

\* Corresponding author: [rmlarose@msu.edu](mailto:rmlarose@msu.edu).

additional depth  $d = O(n^2/\log n)$ . In this paper we introduce a new notion of commutativity which interpolates between these two. The new notion is simply to consider commutativity on blocks of size  $k \in \mathbb{N}$ , and we call this  $k$ -commutativity. For example, we say Paulis  $XXYY$  and  $ZZXX$  two-commute since  $[XX, ZZ] = 0$  (the first two-qubit block) and  $[YY, XX] = 0$  (the second two-qubit block). Qubit-wise commutativity is recovered by  $k = 1$  and (full) commutativity is recovered by  $k = n$ . The advantage, with respect to measuring Hamiltonians, is the potential to reduce measurement complexity by allowing for increased circuit depth in a smooth manner. An example of this is shown in Fig. 1 in which  $k$ -commutativity is applied to measuring the two-dimensional Fermi-Hubbard Hamiltonian. As  $k$  increases, the number of groups decreases, and the value of  $\hat{R}$  (a ratio of the advantage of grouping compared to not grouping, to be defined later) increases, demonstrating reduced measurement complexity.

Although we primarily focus on the application of measurement reduction in this paper, the notion of  $k$ -commutativity may have applications in other areas and so we first introduce it independently in Sec. II. We then describe numerical results for measurement reduction in Sec. III, and finally discuss the asymptotic measurement complexity of  $k$ -commutativity for several families of  $n$ -qubit Hamiltonians in Sec. IV.

## II. $k$ -COMMUTATIVITY

Let  $P = P_0 \otimes \cdots \otimes P_{n-1}$  be an  $n$ -qubit Pauli string. Given integers  $a < b$ , let  $P_{a:b}$  denote  $P$  restricted to  $a$  through  $b - 1$ , i.e.  $P_a \otimes \cdots \otimes P_{b-1}$ . For convenience we consider  $P_a, \dots, P_{-1}$  to be identity if  $a < 0$ , and similarly  $P_n, \dots, P_{b-1}$  to be identity if  $b > n - 1$ . We define  $k$ -commutativity as follows.

**Definition 1** ( $k$ -commutativity). Two  $n$ -qubit Pauli strings  $P = P_0 \otimes \cdots \otimes P_{n-1}$  and  $Q = Q_0 \otimes \cdots \otimes Q_{n-1}$  are said to  $k$ -commute for integer  $1 \leq k \leq n$  if and only if  $[P_{ik:(i+1)k}, Q_{ik:(i+1)k}] = 0$  for all  $i = 0, \dots, \lfloor n/k \rfloor - 1$ . If  $P$  and  $Q$   $k$ -commute, we write  $[P, Q]_k = 0$ .

Note that this definition assumes an ordering of the operators and throughout the paper we consider the ordering to be specified when evaluating  $k$ -commutativity.

As mentioned, we note that  $k = 1$  corresponds to qubit-wise commutativity [6] and  $k = n$  corresponds to full commutativity. Due to its definition,  $k$ -commutativity inherits the usual properties of commutativity. In particular,  $k$ -commutativity is reflexive ( $[P, Q]_k = 0$  implies  $[Q, P]_k = 0$ ) but not transitive (if  $[P, Q]_k = 0$  and  $[Q, R]_k = 0$ , then  $[P, R]_k$  could be zero or nonzero).

Additionally, we prove the following properties.

**Theorem 1:** If  $[P, Q]_k = 0$  then  $[P, Q]_{ck} = 0$  for  $c \in \mathbb{N}$ .

*Proof.* By assumption, in each  $ck$  block of  $P$  and  $Q$  there are  $c$  blocks of  $k$ -commuting strings, thus each block of size  $ck$  commutes.  $\square$

Note that this generalizes from [6] the fact that qubit-wise commutativity implies (full) commutativity. The converse may be true or false — in other words, if  $P$   $k$ -commutes with  $Q$ , we cannot infer whether  $P$   $k'$ -commutes with  $Q$  for  $k' < k$ . The same is true for  $k' > k$  and  $k'$  not a multiple of  $k$ .

Our next properties concern the number of Pauli strings that  $k$ -commute with a given Pauli. For this we show a result for a slightly more general notion of  $k$ -commutativity in which the block sizes can vary. In particular, given two  $n$ -qubit Pauli strings  $P$  and  $Q$ , and  $k_1, \dots, k_m \in \mathbb{N}$  such that  $k_1 + \cdots + k_m = n$ , we say that  $P$  and  $Q$   $(k_1, \dots, k_m)$ -commute if and only if  $[P_{a_j:b_j}, Q_{a_j:b_j}] = 0$  for every  $j = 1, \dots, m$ , where  $b_j = \sum_{\ell=1}^j k_\ell$  and  $a_j = b_j - k_j$ .

**Theorem 2:** Let  $k_1, \dots, k_m \geq 1$  be integers such that  $k_1 + \cdots + k_m = n$ . Then the largest size of a set of  $(k_1, \dots, k_m)$ -commuting  $n$ -qubit Pauli strings, where no two strings are the same modulo phase factors, is  $2^n$ .

*Proof.* First assume that  $m = 2$ , and let  $S$  be a set of the largest possible size of  $(k_1, k_2)$ -commuting  $n$ -qubit Pauli strings, with no two strings same modulo phase factors. Construct the following sets:

$$S_1 := \{P_{0:k_1} : P \in S\}, \quad S_2 := \{P_{k_1:n} : P \in S\}, \quad (3)$$

that is the restriction of the Paulis in  $S$  to the first  $k_1$  qubits, and the next  $k_2$  qubits. We claim that  $S_1$  (resp.  $S_2$ ) is a commuting subset of the  $k_1$ -qubit (resp.  $k_2$ -qubit) Pauli group of the largest possible size, such that there are no two Paulis in  $S_1$  (resp.  $S_2$ ) which are the same modulo phase factors.

We first prove this claim for  $S_1$  (the proof for  $S_2$  is similar). Suppose  $S_1$  is not of the largest possible size. Then there exists a  $k_1$ -qubit Pauli  $P \notin S_1$ , which commutes with all the elements in  $S_1$ , which is also distinct from all the elements in  $S_1$  modulo phase factors. Now pick any  $Q \in S_2$ . Then we have found a new  $n$ -qubit Pauli  $P \otimes Q \notin S$ , which  $(k_1, k_2)$ -commutes with every element in  $S$ . This contradicts the assumption that  $S$  was the largest possible size to begin with.

Now it is known that for any positive integer  $t$ , the largest possible size of a commuting subset of  $t$ -qubit Paulis (modulo phase factors) is  $2^t$  [8, Theorem 1]. Thus we have  $|S_1| = 2^{k_1}$  and  $|S_2| = 2^{k_2}$ . Next, observe that if  $P \in S_1$  and  $Q \in S_2$ , then  $P \otimes Q \in S$ , because  $P \otimes Q$   $(k_1, k_2)$ -commutes with every element in  $S$ , and  $S$  has the largest possible size. This proves that  $|S| \geq 2^{k_1+k_2} = 2^n$ . But  $S$  is also a commuting subset on  $n$ -qubits, and hence by [8, Theorem 1], we must have  $|S| \leq 2^n$ . Combining, we can conclude that  $|S| = 2^n$ .

The general case for  $m > 2$  now follows by iterating this argument.  $\square$

We note an easy consequence of Theorem 2 below:

**Corollary 1:** Let  $k_1, \dots, k_m \geq 1$  be integers such that  $k_1 + \dots + k_m = n$ . Let  $S$  be a set of the largest size of  $(k_1, \dots, k_m)$ -commuting  $n$ -qubit Pauli strings, where no two strings are the same modulo phase factors. For every  $j = 1, \dots, m$ , define  $S_j := \{P_{a:b} : P \in S, b = \sum_{\ell=1}^j k_\ell, a = b - k_j\}$ . Then we have the following:

- (i)  $S' := \{\pm P, \pm iP : P \in S\}$  is a commuting subgroup of the largest possible size of the  $n$ -qubit Pauli group.
- (ii) For every  $j = 1, \dots, m$ ,  $S'_j := \{\pm P, \pm iP : P \in S_j\}$  is a commuting subgroup of the largest possible size of the  $k_j$ -qubit Pauli group.

*Proof.* By the proof of Theorem 2, we already know that  $|S| = 2^n$ , and  $|S_j| = 2^{k_j}$  for each  $j$ . Thus  $|S'| = 2^{n+2}$ , and  $|S'_j| = 2^{k_j+2}$ , by counting all the different phases. It now follows from size considerations [8, Theorem 1, Lemma 4] that  $S'$  is a subgroup of the  $n$ -qubit Pauli group, while  $S'_j$  is a subgroup of the  $k_j$ -qubit Pauli group, for each  $j$ .  $\square$

It is also worth noting the following result that quantifies how many elements of the  $n$ -qubit Pauli group  $(k_1, \dots, k_m)$ -commutes with any given  $n$ -qubit Pauli  $P$  (cf. [8, Lemma 3]):

**Theorem 3:** Let  $P$  be a  $n$ -qubit Pauli string, and let  $k_1, \dots, k_m \geq 1$  be integers such that  $k_1 + \dots + k_m = n$ . Then the number of distinct (up to phase factors)  $n$ -qubit Paulis that  $(k_1, \dots, k_m)$ -commute with  $P$ , including itself, is given by  $4^n / 2^m$ .

*Proof.* For every  $j = 1, \dots, m$ , define  $b_j = \sum_{\ell=1}^j k_\ell$ , and  $a_j = b_j - k_j$ . If  $Q$  is a  $n$ -qubit Pauli that  $(k_1, \dots, k_m)$ -commutes with  $P$ , then for every  $j$ , we have  $[P_{a_j:b_j}, Q_{a_j:b_j}] = 0$ . By [8, Lemma 3], the number of distinct choices (modulo phase factors) for  $Q_{a_j:b_j}$  is  $4^{k_j}/2$ . This gives that the total number of distinct possible choices (modulo phase factors) for  $Q$  is  $\prod_{j=1}^m (4^{k_j}/2) = 4^n / 2^m$ .  $\square$

Our last property concerns the depth of the diagonalization circuit required to measure a set of  $k$ -commuting Paulis. If it were possible to measure all sets of (fully) commuting Pauli strings with a constant depth circuit, there would be no need to consider  $k$ -commutativity with  $k < n$  to reduce the diagonalization circuit depth. Thus we seek a set of commuting Pauli strings which require greater-than-constant circuit depth to measure. The following theorem establishes this.

**Theorem 4:** Consider the gate set  $\{\text{CNOT}, H, S, I\}$  on  $n$ -qubits ( $n \geq 2$ ). Let  $\mathcal{U}$  denote the set of distinct Clifford unitaries that can be obtained by  $d$  applications of gates from this gate set. Then there exists a set of  $r \leq n$  independent commuting  $n$ -qubit Paulis, none of which are

the same modulo phase factors, which are not simultaneously diagonalized upon conjugation by any Clifford in  $\mathcal{U}$ , as long as the following condition holds:

$$d < \frac{\sum_{k=0}^{r-1} \log_2(1 + 2^{n-k})}{\log_2(n^2 + n + 1)}. \quad (4)$$

Note that the minimum depth of an  $n$ -qubit circuit with  $d$  gates is  $\lceil d/n \rceil$ . We prove Theorem 4 in Appendix A.

Last, we note that the procedure for constructing a Clifford circuit to measure a set of  $k$ -commuting Paulis is identical to the case for (full) commutation [2, 9], just with the diagonalization procedure performed in  $\lfloor n/k \rfloor$  blocks of size  $k$  instead of one block of size  $n$ .

### III. MEASUREMENT REDUCTION

To assess measurement reduction from using  $k$ -commutativity to estimate expectation values, we apply the technique numerically to several Hamiltonians. In addition to the Hamiltonian, the tests involve an algorithm to group terms into  $k$ -commuting sets and a metric for the cost. We describe each in turn.

As an initial test we consider the spinless Fermi-Hubbard Hamiltonian

$$H = -t \sum_{\langle i,j \rangle} (a_i^\dagger a_j + a_j^\dagger a_i) + g \sum_{\langle i,j \rangle} a_i^\dagger a_i a_j^\dagger a_j - \mu \sum_i a_i^\dagger a_i \quad (5)$$

on a two-dimensional grid. Here,  $t, \mu, g$  are constants, and  $a_i^\dagger$  (respectively,  $a_i$ ) is the fermionic creation (respectively, annihilation) operator on site  $i$ . The results are shown in Fig. 1 for  $n = 40$  (main plot) and larger values of  $n$  (inset). Here and throughout the paper, we use the sorted insertion algorithm [2] to group terms into  $k$ -commuting sets. This algorithm sorts Hamiltonian terms by coefficient magnitude and then inserts them into  $k$ -commuting sets in a greedy manner (i.e., terms are inserted into the first mutually  $k$ -commuting group available, or inserted into a new group if no such group exists). This results in a number of groups which is plotted in blue in Fig. 1. As can be seen, the number of groups generally decreases as  $k$  increases, although the behavior is not monotonic.

As discussed in [2], the number of groups is not the most suitable metric for evaluating the cost of measuring a Hamiltonian because terms with larger coefficients require more samples to measure. We borrow the example from [2] to illustrate this: letting  $H = 4X_1 + 4X_2 + Z_2 + Z_1X_2$ , the grouping  $\{\{4X_1, Z_2\}, \{4X_2, Z_1X_2\}\}$  results in the smallest number of groups, but the grouping  $\{\{4X_1, 4X_2\}, \{Z_2\}, \{Z_1X_2\}\}$  requires fewer measurements because the terms with large coefficients are in the same group. (For an additional, non-trivial example, see Appendix B.) To quantify this, the authors of [2] intro-

duce the metric

$$\hat{R} := \left[ \frac{\sum_{i=1}^N \sum_{j=1}^{m_i} |c_{ij}|}{\sum_{i=1}^N \sqrt{\sum_{j=1}^{m_i} |c_{ij}|^2}} \right]^2. \quad (6)$$

Here we have arranged the terms into  $N$  groups with  $m_1, \dots, m_N$  Paulis, and  $c_{ij}$  is the coefficient of the  $j$ th Pauli in group  $i$ . This  $\hat{R}$  value has been empirically shown to give a good approximation to the ratio  $R := M_u/M_g$  where  $M_u$  is the number of shots needed to estimate an expectation value to precision  $\epsilon$  without grouping the Pauli strings, and  $M_g$  is the number of shots to estimate the expectation value to precision  $\epsilon$  when the Pauli strings are grouped according to some grouping procedure  $g$  [2]. (Note that  $\epsilon$  does not appear in  $\hat{R}$  because it is a ratio.) The larger  $\hat{R}$  is, the larger the reduction in measurement cost. For the remaining numerical experiments we adopt the  $\hat{R}$  metric (6) to evaluate measurement reduction, but still show the number of groups for context.

Returning to the Fermi-Hubbard experiment in Fig. 1, we see that the  $\hat{R}$  values shown in blue generally increase as  $k$  increases, corresponding to a reduction in shot counts. Compared to  $k = 1$  (qubit-wise commuting), the measurement cost is cut in half for just  $k = 3$  and reduced by more than a factor of ten for  $k = 14$ . Furthermore, we see the interesting property that  $\hat{R}(k)$  attains its maximum at some  $k^* < n$ . In terms of practical experiments, this means that one can measure the energy of this Hamiltonian at the same cost as full commutativity using a diagonalization circuit with fewer gates than the one obtained via full commutativity. To further explore this, we repeat the experiment to find  $k^*(n)$  for  $n = 80$  and  $n = 120$  qubits, and show the results in the inset of Fig. 1. Here, we see  $k^*$  scales linearly with  $n$ , so while there are practical savings in measuring the energy the asymptotics are the same. In Sec. IV we explore this point further and discuss the asymptotics of  $k^*(n)$  for several families of  $n$ -qubit Hamiltonians.

Using the same grouping algorithm and  $\hat{R}$  metric, we test measurement reduction from  $k$ -commutativity for molecular Hamiltonians from HamLib [10] listed in Table I. Each molecule in HamLib includes many Hamiltonian instances, with qubit counts increasing past 100 qubits (*i.e.* many choices of activate space size are available). For this work we choose Hamiltonians of 10 to 16 qubits, testing 11 different molecules from the “standard” subdataset of the electronic structure dataset in HamLib. These molecules are all main group diatomics, where the ccPVDZ basis set and Bravyi-Kitaev encoding were used. The results are shown in Fig. 2. Here, we see a consistent increase in  $\hat{R}$  as  $k$  increases, demonstrating a reduction in cost for measuring expectation values. The reduction in the number of groups is also shown for context. We remark that the measurement reduction obtained by  $k$ -commutativity is similar using the Jordan-Wigner encoding instead of the Bravyi-Kitaev encoding — results are shown in Appendix C.

Molecule	Number of qubits	Number of terms in $H$
O <sub>2</sub>	16	1177
B <sub>2</sub>	10	156
BeH	10	276
BH	10	276
CH	10	276
HF	10	276
C <sub>2</sub>	10	156
OH	10	276
N <sub>2</sub>	14	670
Li <sub>2</sub>	10	156
NaLi	14	1270

TABLE I. Properties of molecular Hamiltonians obtained from HamLib [10] used to test measurement reduction in  $k$ -commutativity (results shown in Fig. 2).

In practical applications, the choice of optimal  $k$  depends largely on the particular quantum computer and overall measurement budget. If the computer is very noisy and one can afford running many circuits, it is best to choose a smaller  $k$  to limit the depth of the diagonalizing circuit. On the other hand if the computer can implement operations with a high fidelity so that a larger diagonalizing circuit could be executed, it is best to choose a larger  $k$  so that the overall measurement complexity is reduced.

#### IV. ASYMPTOTICS OF $k^*(n)$

We now return to the phenomenon in the two-dimensional Fermi-Hubbard model (Fig. 1) in which the value  $\hat{R}(k)$  saturates for some  $k^* < n$ . In this case we see numerically that  $k^*(n)$  scales linearly with  $n$  by repeating the experiment on  $n = 40, 80$ , and 120 qubits. Thus, while  $k$ -commutativity leads to a practical reduction in measurement complexity, the asymptotics are still the same. In this section we consider the question of which Hamiltonians, if any, exhibit a  $k^*(n)$  which scales sublinearly with  $n$ . In particular, we consider several physically inspired models and find examples for which  $k^*(n) = O(1)$  and  $k^*(n) = O(\sqrt{n})$ , the latter case being the same Fermi-Hubbard Hamiltonian in Fig. 1 but using the Jordan-Wigner encoding instead of the Bravyi-Kitaev encoding.

Before analyzing the Fermi-Hubbard model, we first consider if there are physically-inspired classes of  $n$ -qubit Hamiltonians for which  $k^*(n) = O(1)$ . This indeed is true by considering the one-dimensional transverse field Ising model

$$H_n = J \sum_{i=1}^{n-1} Z_i Z_{i+1} + g \sum_{i=1}^n X_i. \quad (7)$$

Here, the  $Z$  type terms in  $H_n$   $k$ -commute for any  $k$ , and similarly for the  $X$  type terms, thus there are exactly two groups for any  $k$  and  $k^*(n) = O(1)$ . Other

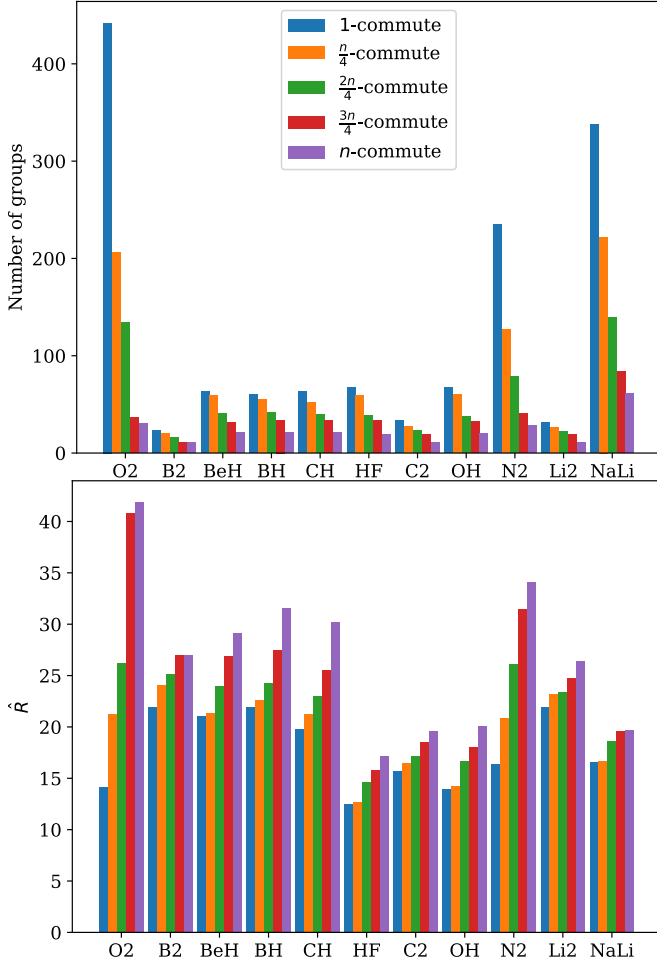


FIG. 2. Results of numerical experiments computing the measurement cost  $\hat{R}$  (6) (bottom panel) and number of groups (top panel) for molecular Hamiltonians listed in Table I. For each molecule we evaluate the measurement cost of  $k$ -commutativity for  $k \in \{1, n/4, n/2, 3n/4, n\}$ . As can be seen  $\hat{R}$  increases as  $k$  increases for all molecules, with the amount varying for different molecules.

cases for which  $k^*(n) = O(1)$  include qubit-based simulation of low-energy Bose-Hubbard models [11–13] and quantum molecular vibrational Hamiltonians [14–16] for which there is a bounded degree of connectivity between vibrational modes. This is because (unlike the case of fermionic commutation) bosonic commutation leads to qubit Hamiltonians with bounded locality.

We now consider the spinless Fermi-Hubbard Hamiltonian (5) under the Jordan-Wigner encoding, starting for simplicity in one dimension. In the Jordan-Wigner encoding, we map the fermion operators  $a_i, a_i^\dagger$  to qubit operators via

$$a_i \rightarrow Z_1 \otimes \cdots \otimes Z_{i-1} \otimes S_i^- \quad (8)$$

$$a_i^\dagger \rightarrow Z_1 \otimes \cdots \otimes Z_{i-1} \otimes S_i^+ \quad (9)$$

where  $S^+ = |1\rangle\langle 0|$  and  $S^- = (S^+)^\dagger$ . The hopping terms

take the form

$$\begin{aligned} a_{i+1}^\dagger a_i &= (Z_1 \otimes \cdots \otimes Z_{i-1} \otimes Z_i \otimes S_{i+1}^+) \\ &\times (Z_1 \otimes \cdots \otimes Z_{i-1} \otimes S_i^- \otimes I_{i+1}) \\ &= Z_i S_i^- \otimes S_{i+1}^+ \\ &= S_i^- \otimes S_{i+1}^+ \end{aligned} \quad (10)$$

and similarly

$$\begin{aligned} a_{i-1}^\dagger a_i &= (Z_1 \otimes \cdots \otimes Z_{i-2} \otimes S_{i-1}^+ \otimes I_i) \\ &\times (Z_1 \otimes \cdots \otimes Z_{i-2} \otimes Z_{i-1} \otimes S_i^-) \\ &= S_{i-1}^+ Z_{i-1} \otimes S_i^- \\ &= S_{i-1}^+ \otimes S_i^- \end{aligned} \quad (11)$$

We then express the raising and lower operators of the spins in terms of Pauli operators

$$S^\pm = \frac{1}{2}(X \pm iY) \quad (12)$$

giving

$$a_{i+1}^\dagger a_i = \frac{1}{2}(X_i - iY_i) \otimes \frac{1}{2}(X_{i+1} + iY_{i+1}) \quad (13)$$

and

$$a_{i-1}^\dagger a_i = \frac{1}{2}(X_{i-1} + iY_{i-1}) \otimes \frac{1}{2}(X_i - iY_i). \quad (14)$$

The strings of the form  $\{X_0 X_1, X_1 X_2, \dots\}$  are qubit-wise commuting, as are  $\{Y_0 Y_1, Y_1 Y_2, \dots\}$ . Observe that

$$[X \otimes Y \otimes I, I \otimes Y \otimes X] = 0. \quad (15)$$

Thus we can build a  $k$ -commuting set  $\{X_0 Y_1, Y_1 X_2, X_2 Y_3, \dots\}$  (for any  $k$ ). Another one can be built by switching  $X$  and  $Y$ . The hopping terms in the Hamiltonian can be sorted into four commuting groups with just  $k = 1$ , regardless of lattice depth.

Next consider Coulomb terms of the form  $a_i^\dagger a_j^\dagger a_i a_j$ . In one dimension, the nearest neighbor points are  $j = i + 1$  and  $j = i - 1$ . Much like with the hopping terms above, these Coulomb terms will only act on neighboring qubits.

$$\begin{aligned} a_i^\dagger a_{i+1}^\dagger a_i a_{i+1} &= (S_i^+ Z_i S_i^- Z_i) (S_{i+1}^+ S_{i+1}^-) \\ &= -S_i^+ S_i^- \otimes S_{i+1}^+ S_{i+1}^- \\ &= -|1\rangle_i \langle 1| \otimes |1\rangle_{i+1} \langle 1| \\ &= -\frac{1}{2}(I_i - Z_i) \otimes \frac{1}{2}(I_{i+1} - Z_{i+1}) \end{aligned} \quad (16)$$

This forms a set of qubit-wise commuting Pauli strings.

Finally, consider an on-site potential term  $a_i^\dagger a_i$ . Again the strings of  $Z$  operators cancel, leaving only operators acting on qubit  $i$ . These can be sorted into  $k$ -commuting groups for any  $k$ . Thus, the whole Fermi-Hubbard Hamiltonian can be sorted into groups with only  $k = 1$ , regardless of the size of the lattice. However, when  $k = 2$ ,

we can sort the terms that go like  $X_i X_{i+1}$  and  $Y_i Y_{i+1}$  into a single group, unlike in the  $k = 1$  case where these terms must go into different groups. Splitting a group of operators into two groups means that  $\hat{R}$  must be less after the splitting [2], so having these  $XX$  and  $YY$  terms in the same group results in a higher  $\hat{R}$ . This can be seen in Fig. 3 on the edges where  $M = 1$  or  $N = 1$  and  $k^*(n) = 2$ . Note that this demonstrates an interesting example where  $k^*(n) = O(1)$  but  $k^*(n) \neq 1$  as in the previously-mentioned Hamiltonians such as the Ising model.

Now consider the two-dimensional case, with lattice size  $M \times N$ . We will use row-major order, *i.e.* the first  $M$  qubits correspond to the first row, the next  $M$  to the second row, etc. Hopping terms between two rows now take the form

$$a_{i+M}^\dagger a_i = S_i^- \otimes Z_{i+1} \otimes \dots \otimes Z_{i+M-1} \otimes S_{i+M}^+ \quad (17)$$

and

$$a_i^\dagger a_{i+M} = S_i^+ \otimes Z_{i+1} \otimes \dots \otimes Z_{i+M-1} \otimes S_{i+M}^- \quad (18)$$

Expanding  $S^\pm$  in terms of Pauli operators, we get Pauli strings of the forms

$$X \otimes Z \otimes \dots \otimes Z \otimes X,$$

$$X \otimes Z \otimes \dots \otimes Z \otimes Y,$$

$$Y \otimes Z \otimes \dots \otimes Z \otimes X,$$

and

$$Y \otimes Z \otimes \dots \otimes Z \otimes Y$$

acting on contiguous blocks of  $M + 1$  qubits. Due to the fact that  $[X, Z] \neq 0$  and  $[Y, Z] \neq 0$ , two Pauli strings must act on completely separate blocks of qubits, and  $k \geq M$ , in order for two strings to commute. For example, the strings  $XZZY$  and  $IXZZY$  do not commute, no matter the block size, as do  $XZZY$  and  $IIXZZY$ . The cutoff value  $k^*$  after which  $\hat{R}$  does not increase should thus be  $M + 1$ . Figure 3 shows the values of  $k^*(M, N)$  computed numerically for various lattices sizes and matches the result  $k^*(M, N) = M + 1$ , or in the case of square lattices that  $k^*(n) = O(\sqrt{n})$ .

The case of the Fermi-Hubbard model in one and two dimensions shows why it is useful to generalize commutation checks beyond the two extreme cases of qubit-wise commutativity and (full) commutativity previously considered in the literature. The energy of the one-dimensional model can be measured using only single-qubit rotations, since all operators are qubit-wise commuting. Previous methods work well in this case. For the two-dimensional model on an  $M \times N$  lattice, we identify a cutoff value  $k^*(M, N) = M + 1$  after which  $\hat{R}$  does not increase. The number of shots needed to measure the energy in this case is thus the same if one uses (fully)  $NM$ -commuting or  $(M + 1)$ -commuting strings. Since fewer

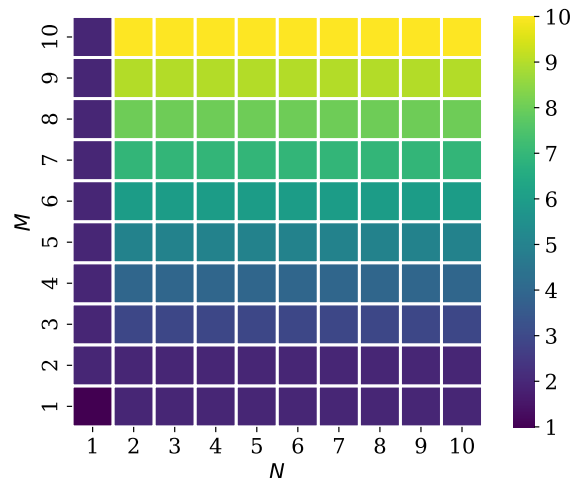


FIG. 3. The values of  $k^*(n) = k^*(M, N)$  for the spinless, aperiodic Fermi-Hubbard Hamiltonian (5) under the Jordan-Wigner transformation on an  $M \times N$  lattice. These values, computed numerically, match the derivation that  $k^*(M, N) = M + 1$  for  $M, N > 1$ , or for square grids that  $k^*(n) = O(\sqrt{n})$ .

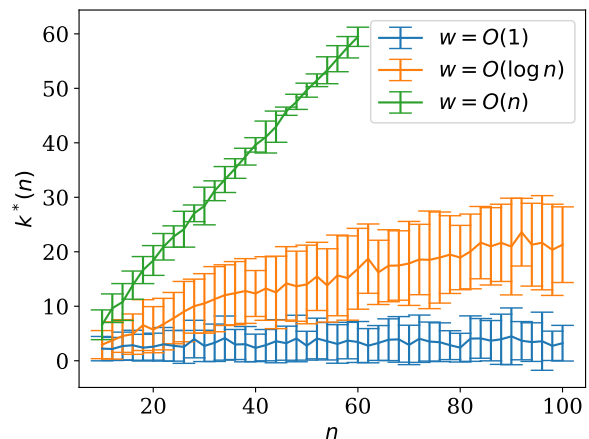


FIG. 4. The values of  $k^*(n)$  for random Hamiltonians. For each  $n$ , a random Hamiltonian  $H_n$  with  $n$  terms is constructed by sampling, for each term, a number of Paulis  $t$  from the exponential distribution  $p(t) = \frac{1}{w} \exp(-wt)$ . Three different values for  $w$  are chosen: constant  $w = 2$ , logarithmic  $w = \ln n$ , and linear  $w = n/2$ . After sampling a number of Paulis  $t$ , each Pauli ( $X$ ,  $Y$ , or  $Z$ ) and each index  $i = 0, \dots, n - 1$  is chosen uniformly at random to form the term. This process repeats for all terms. The value of  $k^*$  is determined as in Fig. 1. Error bars show the standard deviation over fifty random  $H_n$ . As can be seen in the plot of  $k^*(n)$ , the scaling is linear for  $w = O(n)$  and constant for  $w = O(1)$ .

gates are needed to diagonalize the  $(M + 1)$ -commuting sets, the notion of  $k$ -commutativity (here with  $k = M + 1$ ) saves on the total resources (shots and circuit depth) needed to measure the energy.

As a final example, we numerically compute the value of  $k^*(n)$  for random  $n$ -qubit Hamiltonians in one dimen-

sion. To generate these Hamiltonians  $H_n$ , we set the number of terms equal to  $n$ . For each term, a number  $t$  of Paulis is sampled from the exponential distribution  $p(t) = \frac{1}{w} \exp(-wt)$  with parameter  $w$ . Then,  $t$  Paulis  $X, Y, Z$  are chosen uniformly at random, and the qubits that they act on are chosen uniformly at random. Once the Hamiltonian  $H_n$  is constructed,  $k^*(n)$  is numerically computed, and this process repeats for fifty random instances. The results are shown in Fig. 4 for three values of  $w$ , namely constant  $w = 2$ , logarithmic  $w = \ln n$ , and linear  $w = n/2$ . As can be seen in Fig. 4, we observe that the  $k^*(n)$  is linear for  $w = O(n)$  and constant for  $w = O(1)$ . We thus conjecture that random  $n$ -qubit Hamiltonians with a linear number of terms of constant weight are another family of Hamiltonians for which  $k^*(n) = O(1)$ , though we leave a rigorous analysis of this conjecture for future work. One potential application of this conjecture is in error mitigation via quantum subspace expansion [17]. In this framework, one measures the expectation value of an observable projected into the codespace of an error correcting code. By using error correcting codes for which  $k^*(n) = O(1)$ , for example random codes with constant weight stabilizers, one could potentially measure error-mitigated observables with measurement complexity constant or sublinear in  $n$ .

## V. CONCLUSION

In this work we have introduced a simple notion of commutativity for Pauli strings that considers blocks of size  $k \in \mathbb{N}$ , and motivated this notion by the practical application of measurement reduction when evaluating expectation values in quantum circuits. In addition to defining  $k$ -commutativity we have proved several properties of the relation including the size of  $k$ -commuting sets and the depth of diagonalization circuits. Numerically, we have shown a reduction in the measurement complexity of the two-dimensional spinless Fermi-Hubbard model and various molecular Hamiltonians. Finally, we built on an observation in the Fermi-Hubbard model that measurement complexity saturates for some  $k^* < n$  and characterized the asymptotic measurement complexity of  $k$ -commutativity for several families of  $n$ -qubit Hamiltonians.

Our work presents a simple and immediately applicable technique to reduce measurement complexity for many Hamiltonians of interest, and it also opens several lines of future work. First, while we have focused on qubits in this paper, the notion of  $k$ -commutativity can be easily extended to qudits and general operators on a tensor product space. However, when the qudit dimension is not 2, then some of the results obtained in Sec. II will become non-trivial to prove. For example, when the

qudit dimension is composite, it is much harder to establish analogs of the different lemmas used in Appendix A (see [18] to get a sense of how several results for the qudit Heisenberg-Weyl Pauli group is much harder to establish than in the qubit case). Throughout the paper we have fixed an ordering of the qubits when considering  $k$ -commutativity, but it is possible to consider permutations such that larger  $k$ -commuting sets can be formed and measurement complexity can be reduced further (at the cost of introducing SWAP operations in the circuit).

Throughout the work we have also assumed that, when evaluating  $\langle \psi | H | \psi \rangle$ , the depth of the circuit to prepare  $|\psi\rangle$  is comparable to the depth of the circuit to diagonalize (the largest  $k$ -commuting set in)  $H$ . While this seems like a reasonable assumption for many applications and ansatz states  $|\psi\rangle$ , one could imagine scenarios in which a very deep circuit is required to prepare  $|\psi\rangle$  and the depth of the diagonalization circuit is negligible. Our results still apply in this case but the task of finding an optimal  $k$  is less relevant as one would simply choose  $k = n$ . Further, while we have proved a bound on the diagonalization circuit depth, we have done so with respect to Clifford circuits and it's possible that allowing for non-Clifford gates could reduce this bound. To the best of our knowledge this is an open problem in the general context of constructing diagonalization circuits to measure observables. Our bound is also stated in terms of the total number of gates rather than the number of two-qubit gates which could be a more relevant quantity for certain hardware architectures. Last, we have focused exclusively on the  $\hat{R}$  metric which is a reasonable metric for a general setting, but others have been proposed such as Ref. [19] which directly uses the estimation error. While the quantitative advantage of  $k$ -commutativity may differ slightly under other metrics, we still expect the same qualitative behavior.

Overall,  $k$ -commutativity is a simple relation with practical applications in measuring expectation values and potentially in other areas. The idea generalizes and interpolates between two definitions of commutativity — qubit-wise commuting and fully commuting — used when measuring expectation values in quantum circuits. Our work highlights the immediate practical applications while also describing and characterizing interesting properties of  $k$ -commutativity arising in several families of Hamiltonians that can be further pursued in future work.

**Code and data availability** Software to reproduce numerical results can be found in this [Colab](#).

**Acknowledgements** This work was supported by Wellcome Leap as part of the Quantum for Bio Program. RS would like to thank the Institute for Pure and Applied Mathematics for being generous hosts and for providing a great environment during the period when this work was completed.

---

[1] Scott Aaronson and Daniel Gottesman. Improved simulation of stabilizer circuits. *Physical Review A*,

- [2] Ophelia Crawford, Barnaby van Straaten, Daochen Wang, Thomas Parks, Earl Campbell, and Stephen Brierley. Efficient quantum measurement of pauli operators in the presence of finite sampling error. *Quantum*, 5:385, January 2021.
- [3] Aleks Kissinger and John van de Wetering. Pyzx: Large scale automated diagrammatic reasoning. *arXiv preprint arXiv:1904.04735*, 2019.
- [4] Albert T Schmitz, Nicolas PD Sawaya, Sonika Johri, and AY Matsuura. Graph optimization perspective for low-depth trotter-suzuki decomposition. *arXiv preprint arXiv:2103.08602*, 2021.
- [5] Sergey Bravyi, Ruslan Shaydulin, Shaohan Hu, and Dmitri Maslov. Clifford circuit optimization with templates and symbolic pauli gates. *Quantum*, 5:580, 2021.
- [6] Vladyslav Verteletskyi, Tzu-Ching Yen, and Artur F. Izmaylov. Measurement optimization in the variational quantum eigensolver using a minimum clique cover. *The Journal of Chemical Physics*, 152(12):124114, March 2020.
- [7] Abhinav Kandala, Antonio Mezzacapo, Kristan Temme, Maika Takita, Markus Brink, Jerry M. Chow, and Jay M. Gambetta. Hardware-efficient variational quantum eigensolver for small molecules and quantum magnets. *Nature*, 549(76717671):242–246, September 2017.
- [8] Rahul Sarkar and Ewout van den Berg. On sets of maximally commuting and anticommuting pauli operators. *Research in the Mathematical Sciences*, 8(1):14, 2021.
- [9] Pranav Gokhale, Olivia Angiuli, Yongshan Ding, Kaiwen Gui, Teague Tomesh, Martin Suchara, Margaret Martonosi, and Frederic T. Chong.  $\mathcal{O}(n^3)$  measurement cost for variational quantum eigensolver on molecular hamiltonians. 1:1–24, 2020.
- [10] Nicolas PD Sawaya, Daniel Marti-Dafeik, Yang Ho, Daniel P. Tabor, David Bernal, Alicia B. Magann, Shavindra Premaratne, Pradeep Dubey, Anne Matsuura, Nathan Bishop, Wibe A. de Jong, Simon Benjamin, Ojas D. Parekh, Norm Tubman, Katherine Klymko, and Daan Camps. Hamlib: A library of hamiltonians for benchmarking quantum algorithms and hardware, June 2023.
- [11] N Elstner and H Monien. Dynamics and thermodynamics of the bose-hubbard model. *Physical Review B*, 59(19):12184, 1999.
- [12] Rolando Somma, Gerardo Ortiz, Emanuel Knill, and James Gubernatis. Quantum simulations of physics problems. *International Journal of Quantum Information*, 1(02):189–206, 2003.
- [13] Nicolas PD Sawaya. mat2qubit: A lightweight pythonic package for qubit encodings of vibrational, bosonic, graph coloring, routing, scheduling, and general matrix problems. *arXiv preprint arXiv:2205.09776*, 2022.
- [14] Sam McArdle, Alexander Mayorov, Xiao Shan, Simon Benjamin, and Xiao Yuan. Digital quantum simulation of molecular vibrations. *Chemical science*, 10(22):5725–5735, 2019.
- [15] Nicolas PD Sawaya, Gian Giacomo Guerreschi, and Adam Holmes. On connectivity-dependent resource requirements for digital quantum simulation of d-level particles. In *2020 IEEE International Conference on Quantum Computing and Engineering (QCE)*, pages 180–190. IEEE, 2020.
- [16] Pauline J Ollitrault, Alberto Baiardi, Markus Reiher, and Ivano Tavernelli. Hardware efficient quantum algorithms for vibrational structure calculations. *Chemical science*, 11(26):6842–6855, 2020.
- [17] Jarrod R. McClean, Zhang Jiang, Nicholas C. Rubin, Ryan Babbush, and Hartmut Neven. Decoding quantum errors with subspace expansions. *Nature Communications*, 11(11):636, January 2020.
- [18] Rahul Sarkar and Theodore J Yoder. The qudit pauli group: non-commuting pairs, non-commuting sets, and structure theorems. *arXiv preprint arXiv:2302.07966*, 2023.
- [19] Ariel Shlosberg, Andrew J. Jena, Priyanka Mukhopadhyay, Jan F. Haase, Felix Leditzky, and Luca Dellantonio. Adaptive estimation of quantum observables. *Quantum*, 7:906, January 2023.

## Appendix A: Lower bounds on the Clifford gate complexity for diagonalizing commuting Paulis

The goal of this appendix is to establish Theorem 4, repeated here for convenience:

**Theorem 4:** Consider the gate set  $\{\text{CNOT}, H, S, I\}$  on  $n$ -qubits ( $n \geq 2$ ). Let  $\mathcal{U}$  denote the set of distinct Clifford unitaries that can be obtained by  $d$  applications of gates from this gate set. Then there exists a set of  $r \leq n$  independent commuting  $n$ -qubit Paulis, none of which are the same modulo phase factors, which are not simultaneously diagonalized upon conjugation by any Clifford in  $\mathcal{U}$ , as long as the following condition holds:

$$d < \frac{\sum_{k=0}^{r-1} \log_2(1 + 2^{n-k})}{\log_2(n^2 + n + 1)}. \quad (4)$$

The proof uses an elementary counting argument based on some known facts about the Pauli group on  $n$ -qubits, and vector spaces over  $\mathbb{F}_2$ , which we first state below. Recall the definition of the Clifford group  $\mathcal{C}_n$  on  $n$ -qubits:

$$\mathcal{C}_n := \{A \in U(2^n) : APA^\dagger \in \mathcal{P}_n, \forall P \in \mathcal{P}_n\}, \quad (A1)$$

where  $U(2^n)$  and  $\mathcal{P}_n$  are the  $2^n$ -dimensional unitary group and the  $n$ -qubit Pauli group respectively. The first result we need is an exact count of the number of  $n$ -qubit Paulis that are diagonalized by an element of the Clifford group, stated below.

**Lemma 1:** If  $U \in \mathcal{C}_n$ , then all the unique  $n$ -qubit Pauli matrices (upto phase factors) that are diagonalized by  $U$  upon conjugation form a commuting subgroup of  $\mathcal{P}_n$  of size  $2^n$ .

*Proof.* Consider the set of  $n$ -qubit Pauli matrices  $\mathcal{A} := \{X_1, X_2, \dots, X_n, Z_1, Z_2, \dots, Z_n\}$ , which together with  $iI$  generate  $\mathcal{P}_n$ . Here the notation  $X_j$  (resp.  $Z_j$ ) means that we have the Pauli  $X$  (resp.  $Z$ ) on the  $j^{\text{th}}$  qubit, and identities on all the other qubits. It is easily seen that all the elements of  $\mathcal{A}$  are independent as generators of  $\mathcal{P}_n$ . Now for  $j = 1, \dots, n$ , we define

$$P_j := U^\dagger X_j U, \quad Q_j := U^\dagger Z_j U. \quad (A2)$$



Since each element of the Clifford group  $\mathcal{C}_n$  is a commutation preserving group isomorphism of  $\mathcal{P}_n$ , we conclude that the set  $\mathcal{B} := \{P_1, P_2, \dots, P_n, Q_1, Q_2, \dots, Q_n\}$  is also independent, and together with  $iI$  generates  $\mathcal{P}_n$ .

Now define the group  $\mathcal{Q} := \langle Q_1, Q_2, \dots, Q_n \rangle$ . Since for each  $j$ , we have  $UQ_jU^\dagger = Z_j$ , we conclude that for every element  $Q \in \mathcal{Q}$ , the matrix  $UQU^\dagger$  is diagonal. We may also note that  $\mathcal{Q}$  has size  $2^n$ , as it is generated by  $n$  independent elements of  $\mathcal{P}_n$ . Moreover,  $\mathcal{Q}$  is a commuting subgroup because all the generators  $Q_1, \dots, Q_n$  of  $\mathcal{Q}$  commute (this is true since  $Z_1, \dots, Z_n$  commute). It thus remains to show that modulo phase factors, there is no other Pauli  $P \notin \mathcal{Q}$ , such that  $UPU^\dagger$  is diagonal.

To see this, suppose for contradiction that there exists such a Pauli  $P$ , such that  $UPU^\dagger$  is diagonal. Then, as  $P \notin \mathcal{Q}$ , we must have

$$P = \gamma \left( \prod_{j \in J} Q_j \right) \left( \prod_{k \in K} P_k \right), \quad \gamma \in \{\pm I, \pm iI\}, \quad (\text{A3})$$

where  $J, K \subseteq [n] = \{1, \dots, n\}$ , and  $K$  is non-empty. The above equation implies

$$\begin{aligned} UPU^\dagger &= \gamma \left( \prod_{j \in J} UQ_jU^\dagger \right) \left( \prod_{k \in K} UP_kU^\dagger \right) \\ &= \gamma \left( \prod_{j \in J} Z_j \right) \left( \prod_{k \in K} X_k \right), \end{aligned} \quad (\text{A4})$$

which is clearly a contradiction since both  $UPU^\dagger$  and  $\gamma \prod_{j \in J} Z_j$  are diagonal matrices, while  $\prod_{k \in K} X_k$  is not diagonal. This concludes the proof.  $\square$

The next result that we need is an exact count of the number of distinct sets of size  $r \leq n$ , consisting of  $r$  independent commuting elements of  $\mathcal{P}_n$ . We state this in the next lemma, and the proof can be found in [8, Lemma 11].

**Lemma 2:** Let  $n \geq 1$  be the number of qubits. Then the number of distinct sets of  $r$  commuting elements of the Pauli group  $\mathcal{P}_n$ , where no Paulis in the set are the same modulo phase factors, and where all the  $r$  Paulis are independent, is given by

$$\frac{1}{r!} \prod_{k=0}^{r-1} (4^n/2^k - 2^k). \quad (\text{A5})$$

Finally, we recall an well-known result from linear algebra which exactly counts the number of ways to choose  $r$  linearly independent vectors from a  $t$ -dimensional vector space over  $\mathbb{F}_2$ , with  $t \geq r$ :

**Lemma 3:** Let  $t \in \mathbb{N}$ . The number of distinct ways to choose  $r \leq t$  linearly independent vectors from the vector space  $\mathbb{F}_2^t$  is given by

$$\frac{1}{r!} \prod_{k=0}^{r-1} (2^t - 2^k). \quad (\text{A6})$$

We now return to the proof of Theorem 4.

*Proof of Theorem 4.* We first note that we have an upper bound

$$|\mathcal{U}| \leq (n^2 + n + 1)^d, \quad (\text{A7})$$

since every gate can be chosen from the gate set in  $n(n-1) + 2n + 1$  ways. First let us fix any such Clifford unitary  $U \in \mathcal{U}$ . We know by Lemma 1 that modulo phase factors, all the Paulis diagonalized upon conjugation by  $U$  belongs to a commuting subgroup of size  $2^n$ . Let us call this subgroup  $\mathcal{S}$ . As a symplectic vector space,  $\mathcal{S}$  is a  $\mathbb{F}_2$ -vector space of dimension  $n$ . Thus, the number of ways of choosing  $r \leq n$  independent elements of  $\mathcal{S}$ , is the same as choosing  $r$  linearly independent elements of  $\mathbb{F}_2^n$ , and by Lemma 3 this count is given by

$$\frac{1}{r!} \prod_{k=0}^{r-1} (2^n - 2^k). \quad (\text{A8})$$

This count above is exactly the number of sets of size  $r$  consisting of independent commuting Paulis on  $n$  qubits (modulo phase factors), such that all the Paulis in the set are simultaneously diagonalized by  $U$  upon conjugation.

Now by union bound, we may obtain the following upper bound on the number of such sets of size  $r$ , all of whose elements are simultaneously diagonalized upon conjugation by any Clifford unitary in  $\mathcal{U}$ :

$$(n^2 + n + 1)^d \frac{1}{r!} \prod_{k=0}^{r-1} (2^n - 2^k). \quad (\text{A9})$$

On the other hand, we also have from Lemma 2 that the total number of all commuting independent sets of Paulis of size  $r$  (modulo phase factors) is given by the expression in Eq. (A5). Thus to have a set of  $r$  independent Paulis that are not simultaneously diagonalized upon conjugation by any Clifford unitary in  $\mathcal{U}$ , it is a sufficient condition to require that the expression in Eq. (A9) is strictly less than the expression in Eq. (A5); which after simplification yields the equivalent condition

$$\begin{aligned} (n^2 + n + 1)^d &< \frac{\prod_{k=0}^{r-1} (4^n/2^k - 2^k)}{\prod_{k=0}^{r-1} (2^n - 2^k)} \\ &= \prod_{k=0}^{r-1} (1 + 2^{n-k}). \end{aligned} \quad (\text{A10})$$

Taking log base 2 on both sides of the above inequality proves the theorem.  $\square$

## Appendix B: Sorted insertion vs. random insertion

The sorted insertion algorithm [2] works by first sorting the Pauli strings by the absolute values of their coefficients, then sorting them into mutually commuting

groups. Alternatively, the strings could be put into a random order instead of sorting them. The results of this algorithm compared to sorted insertion are shown in Fig. 5. Here, the average number of groups for the randomized algorithm is nearly identical to the number of groups for sorted insertion, with small variance. However, the values of  $\hat{R}$  have large variance, and the average value of  $\hat{R}$  is much lower than sorted insertion. Despite having about the same number of groups, randomization requires many more shots in order to evaluate the same expectation value as sorted insertion.

### Appendix C: Additional numerical results

Here we include additional numerical results, in particular the analogue Fig. 2 using the Jordan-Wigner encoding is shown in Fig. 6, and the analogue of Fig. 3 using the Bravyi-Kitaev encoding is shown in Fig. 7.

For the molecular Hamiltonians (Fig. 6), we see comparable results to Fig. 2. The behavior that  $\hat{R}$  increases as  $k$  increases is still seen and the vertical axis is on the same scale, but for some molecules  $\hat{R}$  seems to increase more quickly under than Bravyi-Kitaev encoding than the Jordan-Wigner encoding, notably  $O_2$  and  $B_2$ .

For the Fermi-Hubbard model (Fig. 7), the behavior of  $k^*(n)$  under the Bravyi-Kitaev encoding is qualitatively similar to the case of the Jordan-Wigner encoding (Fig. 3), however the pattern is less regular and the values are generally higher.

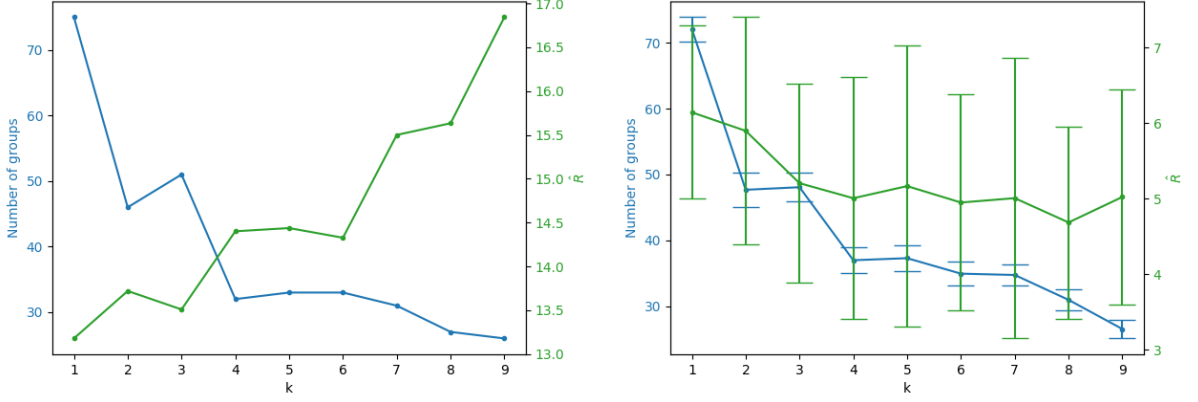


FIG. 5. The number of groups and  $\hat{R}$  metrics obtained for sorted insertion (left panel) and random insertion (right panel) on the  $n = 10$  qubit  $C_2$  molecule [10]. For random insertion, error bars show the standard deviation over 100 trials. Note that the number of groups is comparable for both algorithms but the values for  $\hat{R}$  are substantially different. In particular,  $\hat{R}$  is significantly lower for the random insertion algorithm. This, as well as the relatively large variance in  $\hat{R}$  for the random insertion algorithm, provides another example showing that  $\hat{R}$  is a more appropriate metric than the number of groups.

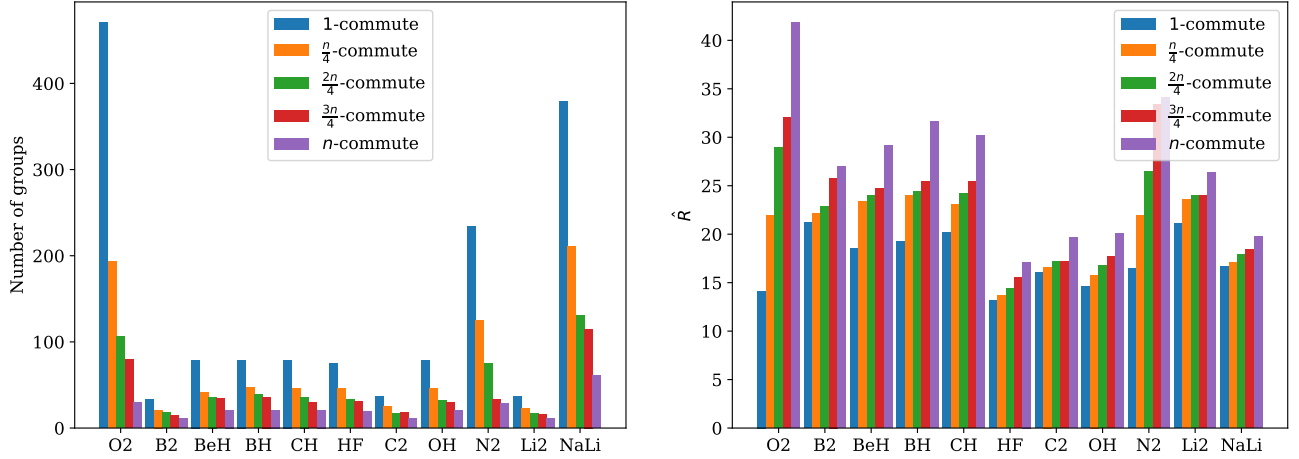


FIG. 6. The same as Fig. 2 but using the Jordan-Wigner encoding instead of the Bravyi-Kitaev encoding.

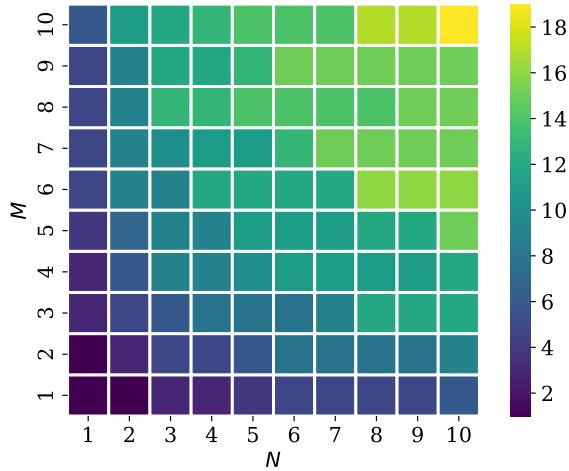


FIG. 7. The same as Fig. 3 but using the Bravyi-Kitaev encoding instead of the Jordan-Wigner encoding.